



## Non-fluorinated sol-gel processing of hydrophobic coating on cotton fabric

M Zakerizadeh<sup>1</sup>, M Akbari Dogolsar<sup>1,a</sup>, Z Jamshidi<sup>2</sup> & A K Haghi<sup>1</sup>

<sup>1</sup>Department of Textile Engineering, Faculty of Engineering, University of Guilan, Rasht, Iran

<sup>2</sup>Department of Textile Engineering, Isfahan University of Technology, Isfahan, 84156-83111, Iran

Received 1 March 2021; revised received and accepted 25 June 2021

In this study, the importance of wash durability tests for providing efficient hydrophobic surfaces through non-fluorinated sol-gel processes has been investigated. Various concentrations of methyltriethoxysilane (MTEOS) and trimethylchlorosilane (TMCS) have been used to deposit SiO<sub>2</sub> nanoparticles on a cotton fabric in a two-step sol-gel process. The effects of catalyst type on the hydrophobic properties of fabric are investigated by using ammonia or hydrochloric acid in the sol-gel procedure. Surface characteristics, such as morphology and wettability are evaluated by image processing techniques and contact angle measurements. Air permeability, mechanical strength and wash durability tests are also performed to investigate the physical/mechanical properties of the samples. The results show that SiO<sub>2</sub> nanoparticles are well dispersed on cotton fabrics with a contact angle of 149°. It is revealed that the fabric coated with 1 mL of MTEOS and ammonia catalyst exhibits the highest breathability and strength. Moreover, the first stage of the sol-gel technique is sufficient to provide super hydrophobicity. However, the results of the durability test indicate that sol-gel technique does not provide suitable wash durability that should be considered in future investigations.

**Keywords:** Biocompatible coating, Cotton fabric, Hydrophobic coating, Silica film, Sol-gel method

### 1 Introduction

The fabrication of artificial hydrophobic surfaces was firstly inspired by microstructures of lotus leaf<sup>1</sup>. With introduction of scanning electron microscopy in the 1960s, the hierarchical surface morphology of the lotus leaf was observed. Owing to the presence of microscale protrusions on a macroscale smooth surface, lotus leaves exhibit superhydrophobic properties and self-cleaning abilities. The advances made in surface modification techniques enable superhydrophobic surfaces to be used in a wide range of applications<sup>2, 3</sup> such as touch displays of smart phones, anti-fogging glass, solar panels and in textile industries. A single droplet on such a hydrophobic surface shows a high contact angle between 90° and 180° (refs 4, 5). The advantages of self-cleaning coatings range from short cleaning time, low maintenance costs, and high durability<sup>6</sup>. In a hydrophobic coating, two factors should be considered, namely the surface roughness and surface energy. Without any nano- or micro-structure, it is impossible to achieve a contact angle greater than 120° on a smooth surface with low surface energy. Therefore, surface roughness should also be

considered as an important factor affecting the hydrophobic properties<sup>7</sup>. Previous research studies<sup>8-12</sup> have used various surface modification techniques, such as electrochemical deposition, lithography, chemical vapor deposition, electrospinning and sol-gel. The sol-gel method is one of the most preferred techniques due to its simple process, low cost, high product yield, low processing temperature, safety and simple equipment. Previous researchers have used different materials, such as glass, aluminum and textile fabric modified by different methods to achieve a hydrophobic surface<sup>13-16</sup>. For instance, Basu *et al.*<sup>17</sup> investigated the hydrophobic properties of two nanocomposite coatings produced by two different precursors (MTEOS and TEOS) and hexamethyldisilazane (HMDS) modifier. The results showed that MTEOS precursor improves the superhydrophobic properties with a contact angle of 166°. Moreover, increasing the amount of modifier enhances the hydrophobicity. Lakshmi *et al.*<sup>18</sup> prepared a superhydrophobic coating with improved hardness by embedding fumed silica nanoparticles in a condensed hybrid sol of MTEOS and colloidal silica. By comparing the hydrophobic properties of a surface using two different modifiers (TMCS and HMDS), it was concluded that TMCS could provide moisture and heat resistant surfaces with greater

<sup>a</sup>Corresponding author.  
E-mail: akbari@guilan.ac.ir

contact angles<sup>19-21</sup>. In another research, HMDS modifier was used to prepare a hydrophobic cotton fabric with a contact angle of 110° (ref. 17). Shi *et al.*<sup>18</sup> prepared a superhydrophobic cotton fabric coated by TiO<sub>2</sub> and modified by Octadecyl thiol (ODT) with a contact angle of 151°. Zhang *et al.*<sup>22</sup> used layer-by-layer self-assembly procedure to prepare superhydrophobic cotton fabric. Cationic poly (dimethyldiallylammonium chloride) and negative charged silica nanoparticles were coated on the fabric and modified by (heptadecafluoro-1,1,2,2-tetradecyl) trimethoxysilane to achieve a superhydrophobic surface with a contact angle of 155°. Colleoni *et al.*<sup>23</sup> fabricated hydrophobic cotton and polyester fabrics by hydrolysis and condensation of octyltriethoxysilane (OTES) combined with a melamine based crosslinking agent. Das *et al.*<sup>24</sup> prepared a superhydrophobic cotton fabric with a contact angle of 163° to be used in a water/oil separation system with a high efficiency of 98.8%.

Prior studies have used fluorinated materials to provide hydrophobic surface coating. Nevertheless, biocompatibility of the coating material has been a major concern for the end application. For clothing applications, breathability and sufficient stability of the coating material should also be considered. Therefore, the main objective of the present work is to investigate the breathability and washing durability of a biocompatible hydrophobic surface prepared by a non-fluorinated sol-gel method. Methyltriethoxysilane (MTEOS) and trimethylchlorosilane (TMCS) are used, in different concentrations, as precursor and modification agent respectively, to deposit SiO<sub>2</sub> nanoparticles on the cotton fabric in two-step sol-gel process. Surface morphology, wettability, air permeability, mechanical strength and wash durability have been investigated through several tests. Since few research studies have been done to investigate the effects of catalyst type on the surface hydrophobicity, ammonia and hydrochloric acid were used, separately, in the sol-gel procedure.

## 2 Materials and Methods

### 2.1 Materials

Methyltriethoxysilane (MTEOS), trimethylchlorosilane (TMCS), ethanol 96%, hydrochloric acid 37%, and ammonia 25% were all purchased from Merck (Darmstadt, Germany). 100% cotton fabrics were plain woven on a weaving machine (Behbaft Co., Guilan). All samples were made from 20 Ne warp and weft yarns with 24 and 23 picks/cm

respectively. The woven fabric was cut into small pieces (2.5×3 cm<sup>2</sup>).

### 2.2 Preparation of Hydrophobic Coating

A schematic of the processing stages used for fabrication of hydrophobic surface is represented in Fig. 1. Considering the main reactions in sol-gel process, as mentioned by previous research studies<sup>25</sup>, similar approach was used to prepare the sols in the present work. In the first stage, different solutions of 1.14 mL of ethanol mixed with different amounts of MTEOS (0.5, 1 and 2 mL) were prepared and then stirred with a magnetic stirrer at 25°C for 3 min. Then, the catalyst (ammonia or hydrochloric acid) was added drop-wise into the solutions and stirred for 48 h. When the hydrolysis and condensation procedures were fully performed, the white sols were obtained. Afterwards, the woven samples were dipped in the solutions for 15 min and dried at 20°C. During curing and drying period, the hydroxyl groups of cellulose could be substituted by the alkyl groups of hydrophobic coating material. Finally, a hydrophobic cotton fabric coated by nanoparticles could be obtained.

After the first stage, using the field emission scanning electron microscopy (FESEM) images of the samples and image processing technique, the distribution and uniformity of the nanoparticles were compared. Based on contact angle measurements (illustrated in next sections) and nanoparticle size/distribution, the most appropriate condition was considered for the next stage investigations. In the second stage, different colloidal mixtures of ethanol and TMCS with different volumetric ratios (TMCS to ethanol = 2.5, 5 and 7.5 vol%)<sup>26</sup> were prepared and stirred for 30 min at 25°C. The woven samples dip coated by MTEOS/Ethanol solution was immersed in the TMCS/ethanol mixtures for 1 min. Then, the samples were placed in an oven for 2 min at 150°C. The characteristics of sol-gel solutions are presented in Table 1.

### 2.3 Characterization of Surface Morphology

A scanning electron microscope (MIRA3, TESCAN Co.) under the voltage of 20 kV was used to investigate the surface characteristics, such as nanoparticle size and distribution. Energy dissipation spectroscopy (EDS) analysis was conducted to confirm the elemental composition.

### 2.4 Contact Angle Measurement

Contact angle was measured by a Protractor device (10-CAG Goniometer Angle Contact). A distilled water droplet with the volume of 5 µL was placed on

the surface of sample. Images of a water droplet were magnified and displayed by a CMOS camera and the contact angle was determined using Image J software.

### 2.5 Droplet Adsorption Time

The droplet adsorption time was estimated for each sample, according to the standard AATCC 79-2000 Test Method. Four droplets were placed on different parts of the sample and the average of observations was reported as the average droplet adsorption time.

### 2.6 Wash Durability Test

The standard ISO 3175 test method was used to evaluate the durability of the coated samples. The samples were washed in a dilute anionic detergent solution (1 g/L and L:M ratio = 40:1) at 30°C for 10 min. Then, the samples were rinsed and dried at 20°C

### 2.7 FTIR Spectroscopy

FTIR analysis was used to investigate the chemical bonds between the coated layer and the fabric surface.

The FTIR spectra were recorded by a spectrometer device (Nikolet Magan-IR 560) in the transmission mode between  $411\text{ cm}^{-1}$ - $4111\text{ cm}^{-1}$  at 25 °C.

Table 1 — Compositions of sol-gel solutions, deposited on to the cotton substrates

Sample	Stage 1				Stage 2 TMCS/Ethanol % vol
	MTEOS mL	Ethanol mL	Catalyst		
			Ammonia M	HCL M	
1	-	-	-	-	-
2	0.5	1.14	2	-	-
3	1	1.14	2	-	-
4	2	1.14	2	-	-
5	0.5	1.14	-	0.1	-
6	1	1.14	-	0.1	-
7	2	1.14	-	0.1	-
8	1	1.14	2	-	2.5
9	1	1.14	2	-	5
10	1	1.14	2	-	7.5

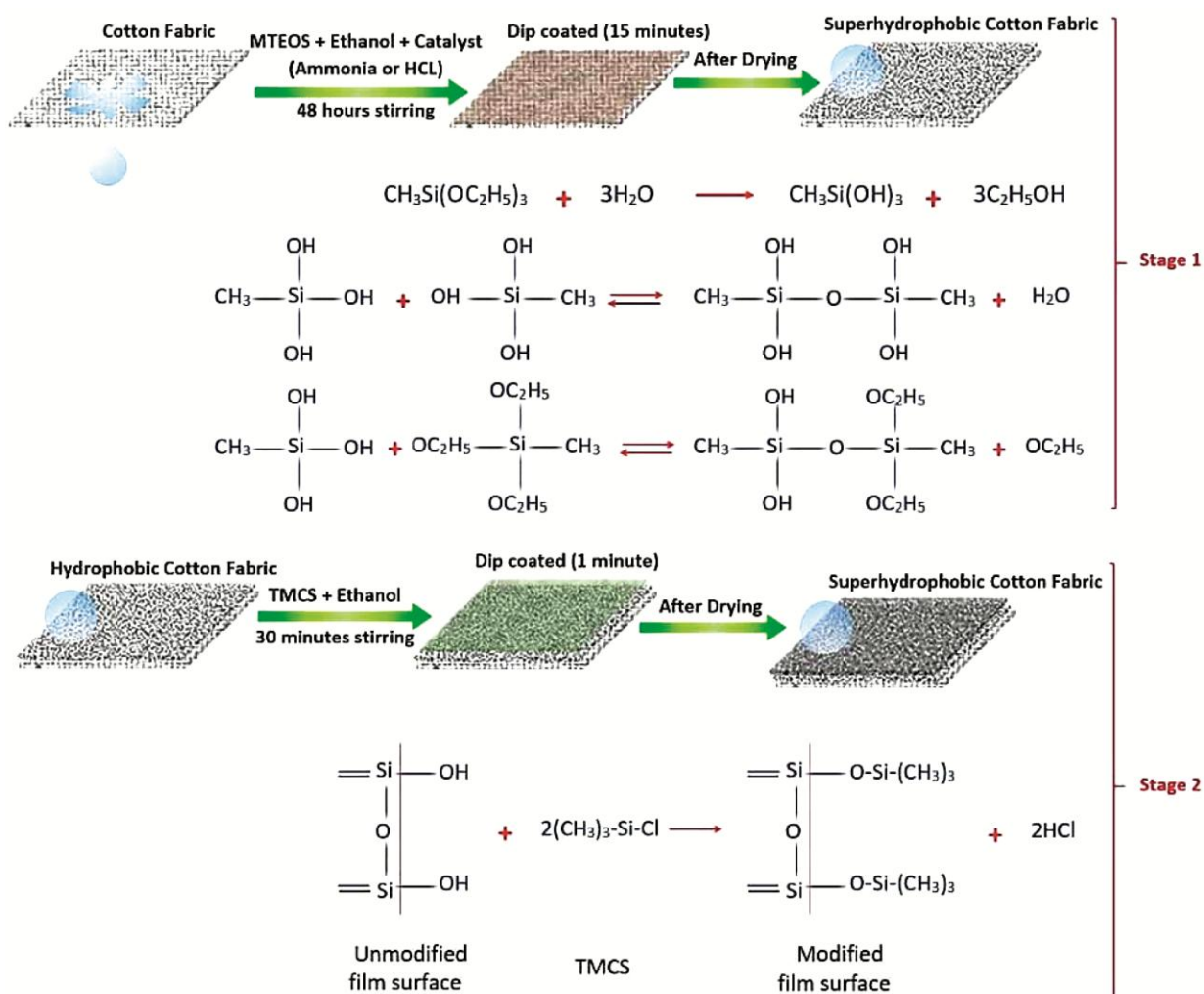


Fig. 1 — Two-stage fabrication of superhydrophobic coating on cotton fabric and sol-gel reactions

### 2.8 Mechanical Tensile Test

According to the ASTM D5034-95 standard test method, mechanical tensile tests (tensile strength and % elongation) were performed to investigate the tensile properties of the samples by the use of tensile test device (Co. Shirley, England) at 23°C and 43% RH.

### 2.9 Air Permeability

The permeability of the samples was measured by the use of a FX 3300 (Switzerland) apparatus under the air pressure of 125 Pa, according to the ASTM D737-96 standard test method.

## 3 Results and Discussion

### 3.1 Surface Characterization

Figure 2 represents the FESEM images of the pristine cotton fabric and the coated samples in both stages. The results of image analysis indicate that the nanoparticles with diameters in the range of 36 nm and 46 nm are formed successfully on the surface of cotton fibers. As shown in Table 2, considering the nanoparticles size/distribution together with the contact angle measurements, the appropriate coating condition belongs to the sample with 1 mL of MTEOS when ammonia is used as the catalyst solution.

The nanoparticle size increases with increasing the amount of MTEOS. The most uniform distribution of nanoparticles belongs to the sample fabricated with 1 mL of MTEOS and a basic catalyst solution of ammonia. When ammonia catalyst is used, the size of nanoparticles is found larger than that when hydrochloric acid is used. The surface contact angle strongly depends on the particle size and distribution. Higher amounts of nanoparticles with large diameters and uniform distributions provide greater contact angles<sup>27</sup>. Therefore, the solution prepared with ammonia and 1 mL of MTEOS is considered as the appropriate solution for the next investigations. In the second stage, nanoparticles with diameter in the range of 42 - 62 nm are formed successfully on the surface of cotton fibres.

The nanoparticle size also increases with increasing the TMCS/ethanol volumetric ratio. According to the theory of Rao *et al.*<sup>23</sup>, with increasing the nanoparticle size, a decreasing trend is observed in the nanoparticle population on the surface of fibers. It is due to the fact that in higher volumetric ratios, free nanoparticles with no attachment or chemical bond are formed on the surface of fibres.

### 3.2 Contact Angle Measurements

Figure 3 (a) shows the results of contact angle measurements for the samples prepared in the first stage. According to the results, the highest values of contact angles belong to the Samples 3 and 6 fabricated with 1 mL of MTEOS. The increase in contact angle from 143° to 146.1° is attributed to the increase of the precursor and the number of methyl groups attached to the silica surface<sup>28</sup>. However, higher amounts of the precursor results in the saturation of methyl groups and formation of molecular irregularities, which reduce the contact angle<sup>26</sup>. It can be seen that the samples prepared with ammonia catalyst solution exhibit greater contact angles than the samples catalyzed by HCL solution. As described by previous researchers<sup>26, 28</sup>, the condensation and hydrolysis reaction occur simultaneously in the basic conditions. In other words, in acidic conditions, the formation of a strong network structure is limited. In basic conditions, the cross-linking occurs between the networks and forms a dense and porous structure. Figure 3 (b) shows the results of contact angle measurements for the samples prepared in the second stage.

According to the results, the highest value of contact angles belongs to the Samples 9 fabricated with 5 % vol of TMCS/ethanol. The increase in contact angle from 144.37° to 149° is attributed to the increase of the precursor and the number of Si-(CH<sub>3</sub>)<sub>3</sub> groups attached to the silica surface<sup>26</sup>. However, higher amounts of the precursor results in the saturation of Si-(CH<sub>3</sub>)<sub>3</sub> groups and formation of molecular irregularities which reduces the contact angle<sup>19</sup>.

In another work, Mohamed *et al.*<sup>24</sup> indicated that superhydrophobicity, described by the contact angles above 150°, shows a nearly perfect non-wetting state<sup>27</sup>. Herein, it can be seen that Sample 9 with the contact angle of 149° (~ 150°) is almost a superhydrophobic surface. According to the results, the contact angle of Sample 3 (146.1°) is also great enough (~ 150°) to describe hydrophobicity (the sample prepared in the first stage with ammonia solution and 1 mL of MTEOS). Therefore, it can be concluded that the first stage of the sol-gel technique is sufficient to provide superhydrophobicity and there is no need to perform the second stage.

### 3.3 Droplet Adsorption Time

Figures 4 (a) and (b) represent the results of droplet adsorption test and the time required for a single droplet to pass through the samples.

The trends observed for the results of droplet adsorption time are found the same as the trends obtained from the results of contact angle measurements for different samples. It means that the

maximum droplet adsorption time in the first stage belongs to Sample 3 (ammonia + 1 mL of MTEOS) and in the second stage, the maximum time belongs to Sample 9 (5 % vol. of TMCS/Ethanol).

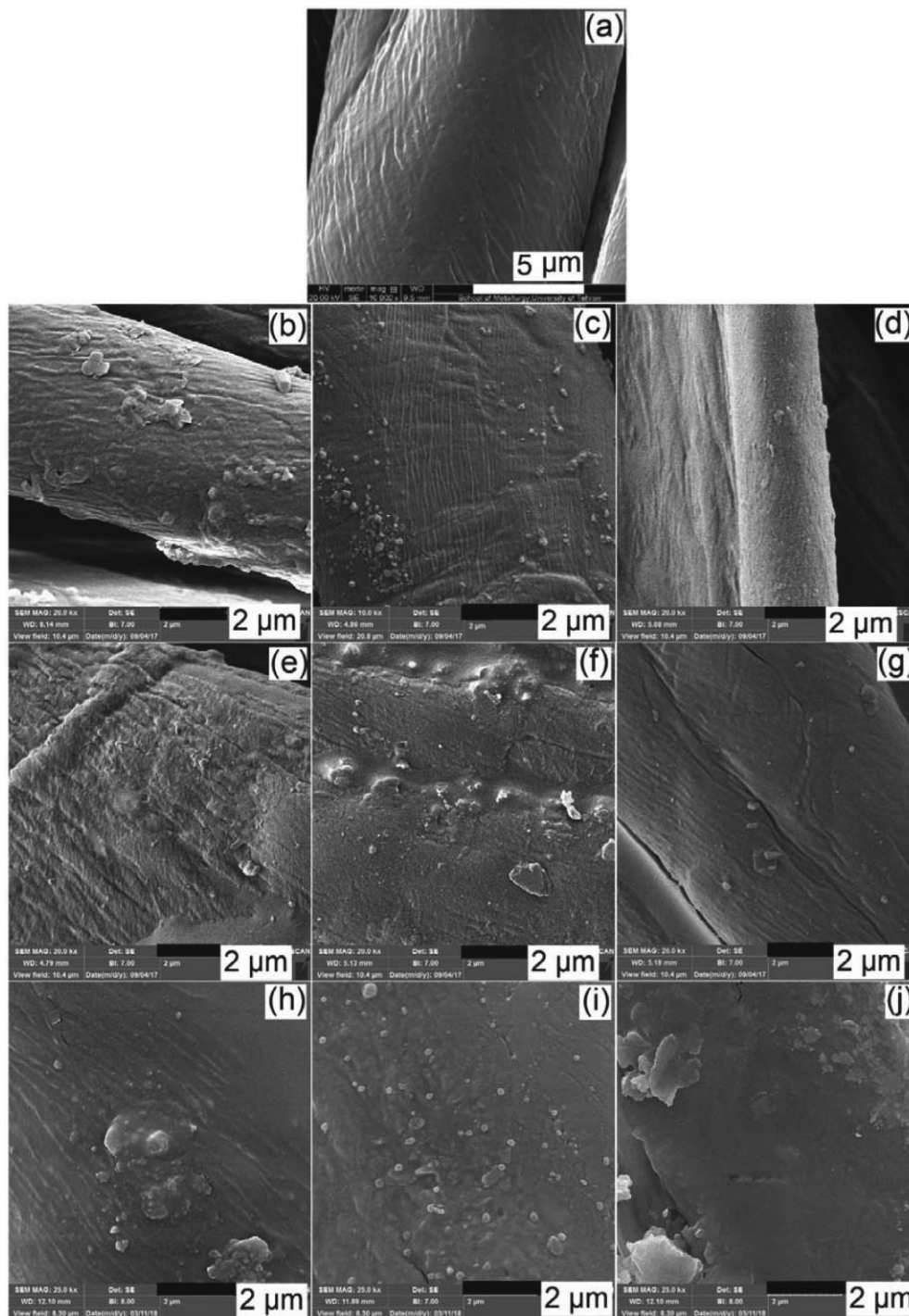


Fig. 2 — FESEM images of the samples with different amounts of MTEOS/different catalysts and of the samples modified in the second stage with different TMCS/ethanol volumetric ratio (a) Sample 1 (the pristine sample), (b) Sample 2 (0.5 mL, ammonia), (c) Sample 3 (1 mL, ammonia), (d) Sample 4 (2 mL, HCL), (e) Sample 5 (0.5 mL, HCL), (f) Sample 6 (1 mL, HCL), (g) Sample 7 (2 mL, HCL), (h) Sample 8 (2.5 % vol), (i) Sample 9 (5 % vol) and (j) Sample 10 (7.5 % vol).

Table 2 — Nanoparticle size and distribution in different samples

Sample code	Nanoparticle size nm	Standard deviation, nm
2	36.50	14.93
3	46.75	10.13
4	43.17	25.60
5	36.89	9.76
6	40.72	6.20
7	36.23	10.74

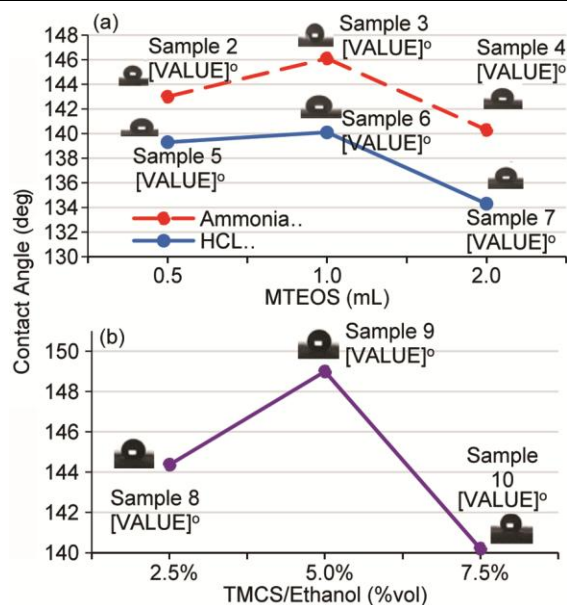


Fig. 3 — Comparison of measured contact angles of the samples prepared (a) in first stage with different amounts of MTEOS (0.5, 1 and 2 mL) and different catalysts (ammonia or HCL), and (b) in the second stage with different TMCS/ethanol volumetric ratios (2.5, 5 and 7.5 % vol)

### 3.4 Wash Durability Test

The standard test method of ISO 3175 has been used to investigate the wash durability of the samples prepared with different conditions. Herein, 5 cycles are performed according to the standard test method. After each washing cycle and drying procedure, the contact angle and drop adsorption time measurements are conducted again on all samples. After 3 cycles, the most changes are observed in the hydrophobic characteristics. No significant change is observed among cycles 3, 4 and 5. As shown in Fig. 4 (c), 18% and 21% reduction in hydrophobic characteristics (contact angle and drop adsorption time) is observed for the samples prepared in the first stage and second stage respectively. The significant fall in the contact angles after the first three washes can be attributed to the presence of physical interaction between coating material and cotton fabric. Therefore, it can be concluded that besides the excellent super-

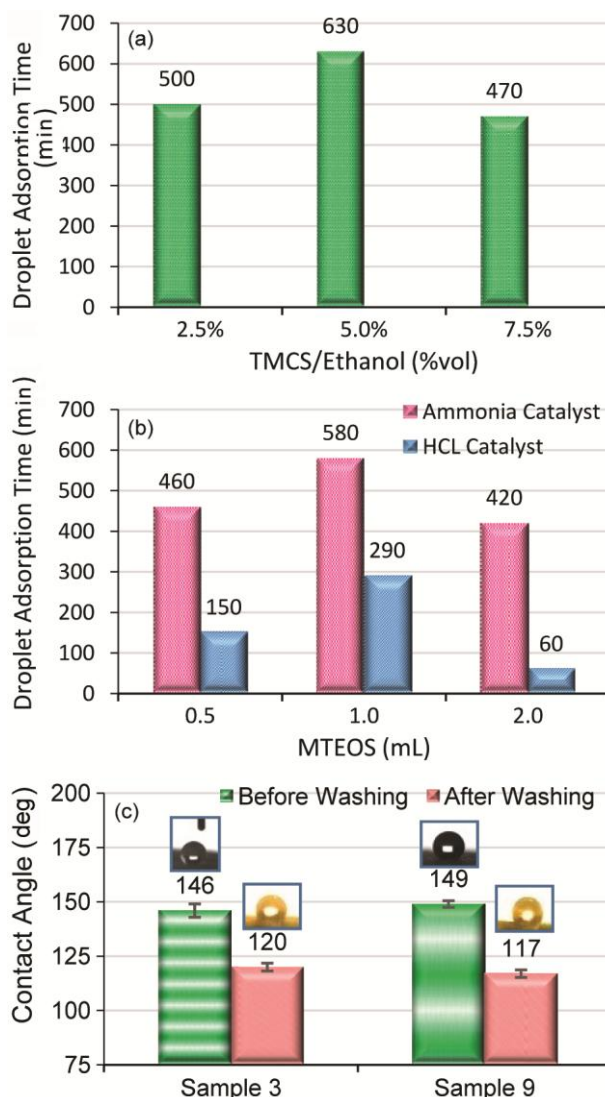


Fig. 4 — Drop adsorption time for (a) samples prepared in the first stage with different amounts of MTEOS (0.5, 1 and 2 mL) and different catalysts (ammonia or HCL); (b) samples prepared in the second stage with different TMCS/ethanol volumetric ratios (2.5, 5 and 7.5 % vol), (c) the contact angles of the samples 3 (1<sup>st</sup> stage: ammonia + 1 mL of MTEOS) and 9 (2<sup>nd</sup> stage: 5 % vol of TMCS/ethanol) before and after wash durability test

hydrophobic properties of the samples, even the first stage is not capable to provide an appropriate hydrophobic surface with sufficient durability. Therefore, especially in clothing applications, the washing durability tests should also be performed to investigate the efficiency of superhydrophobic coatings in laundry conditions.

### 3.5 EDX Analysis

The spectra and quantitative results of the EDX analysis are presented in Table 3 and Figs 5 (a) and (b) respectively. The EDX analysis for a pristine

Table 3 — Quantitative results of EDX analysis for Sample 2 [1<sup>st</sup> stage: MTEOS (1 mL) + ammonia] and Sample 9 [1<sup>st</sup> stage: MTEOS (1 mL) + ammonia, and 2<sup>nd</sup> stage: TMCS/ethanol (5 % vol)]

Sample 2		Sample 9		Element
Weight %	Atomic %	Weight %	Atomic %	
38.04	45.85	38.88	46.93	Carbon
57.05	51.62	55.26	50.07	Oxygen
4.91	2.53	5.55	2.86	Silicon
0	0	0.32	0.13	Chlorine

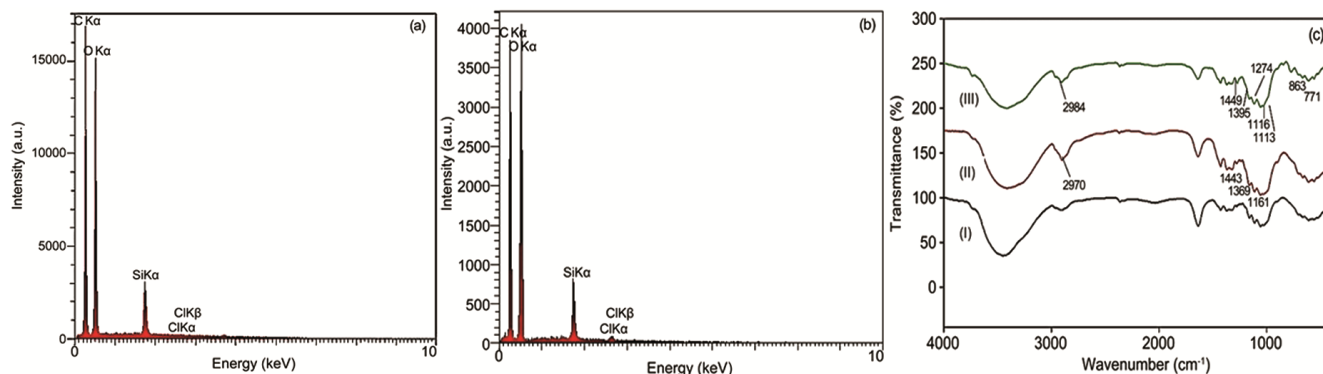


Fig. 5 — EDX spectra for (a) Sample 2 [1<sup>st</sup> stage: MTEOS (1 mL) + ammonia], and (b) Sample 9 [1<sup>st</sup> stage: MTEOS (1 mL) + ammonia, 2<sup>nd</sup> stage: TMCS/ethanol (5 % vol)]. FTIR spectra (c) of different samples (I) Sample 1 (pristine cotton fabric), (II) Sample 3 (1<sup>st</sup> stage: ammonia + 1 mL of MTEOS) and (III) sample 9 (2<sup>nd</sup> stage: 5 % vol of TMCS/ethanol)

cotton fabric shows two types of elements, viz carbon and oxygen<sup>29</sup>. However, in the Sample 2, silicon is also observed in addition to carbon and oxygen. The presence of chlorine in Sample 9 denotes the TMCS compound. Except oxygen, all other elements in Sample 9 are observed in higher percentages as compared to the elements of Sample 2.

### 3.6 FTIR Analysis

The FTIR spectra of pristine cotton fabric, Sample 3 (1<sup>st</sup> stage: ammonia + 1 mL of MTEOS) and Sample 9 (2<sup>nd</sup> stage: 5 % vol of TMCS/ethanol) are presented in Fig. 5 (c). The wave numbers of 2970 cm<sup>-1</sup> and 2984 cm<sup>-1</sup> are attributed to the symmetric and asymmetric tensile vibrations of CH<sub>2</sub> groups. The CH<sub>3</sub> groups in the first stage (MTEOS) and second stage coating (TMCS) are observed at wave numbers of 1443 cm<sup>-1</sup>, 1369 cm<sup>-1</sup>, 1449 cm<sup>-1</sup>, 1395 cm<sup>-1</sup><sup>30, 31</sup>. The peaks observed at 1274 cm<sup>-1</sup>, 771 cm<sup>-1</sup> and 863 cm<sup>-1</sup> denote the tensile vibrations of C-Si-CH<sub>3</sub> and Si-CH<sub>3</sub> due to the presence of MTEOS, which is increased in the second stage. The main characteristic peaks at 1161 cm<sup>-1</sup>, 1113 cm<sup>-1</sup>, 1116 cm<sup>-1</sup> are attributed to the Si-O-Si groups<sup>22, 23, 29</sup>. The broad absorption bands at around 1649 and 3330 cm<sup>-1</sup> indicate the presence of hydroxyl groups<sup>32</sup>. The decrease in absorbance peak at 3330 cm<sup>-1</sup> and 800 cm<sup>-1</sup> is attributed to the OH groups of cellulose<sup>32, 33</sup>, which is reacted with the

coating of sols and condensed with the alkyl groups. The FTIR results indicate that MTEOS and TMCS-based coatings with alkyl groups (without polar groups) are capable to chemically substituted with hydrophilic groups of cellulose and provide hydrophobicity.

### 3.7 Longitudinal and Transverse Tensile Strength

Figure 6 (a) represents the longitudinal and transverse tensile strength of the Sample 1 (pristine cotton fabric), Sample 3 (1<sup>st</sup> stage: ammonia + 1 mL of MTEOS) and Sample 9 (2<sup>nd</sup> stage: 5 % vol of TMCS/ethanol). The results show that no significant change occurs in the tensile strength of samples in both directions. However, there is a significant reduction trend in the strength of Sample 9 (prepared in the second stage) that could be due to the release of the chlorine atoms which could reduce the strength of the cotton fabric<sup>30, 31, 34</sup>.

### 3.8 Air Permeability

Air permeability is one of the most important properties of a fabric and depends on the porosity of the fabric. Figure 6 (b) represents the results of air permeability for Sample 1 (pristine cotton fabric), Sample 3 (1<sup>st</sup> stage: ammonia + 1 mL of MTEOS) and Sample 9 (2<sup>nd</sup> stage: 5 % vol of TMCS/ethanol). It is obvious that non-coated fabrics due to their low thicknesses and high porosities, show higher

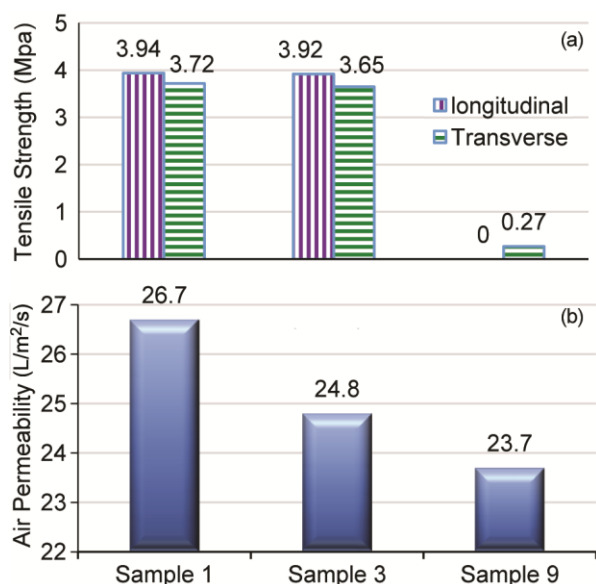


Fig. 6 — (a) Longitudinal and transverse tensile strength and (b) air permeability of Sample 1 (pristine cotton fabric), Sample 3 (1<sup>st</sup> stage: ammonia + 1 mL of MTEOS) and Sample 9 (2<sup>nd</sup> stage: 5 % vol of TMCS/Ethanol)

permeability in comparison to the coated fabrics<sup>35</sup>. Herein, the 7.1% and 11.9% reductions are observed in the permeability of the pristine cotton fabric after being coated in the first and second stage respectively. As the observed changes are not significant, especially in the first stage, it can be concluded that the breathability of the samples could be preserved after being coated in the first stage.

#### 4 Conclusion

A superhydrophobic cotton fabric is fabricated through a two-step sol-gel process. Various concentrations of MTEOS and TMCS are used as precursor and modification agent to deposit SiO<sub>2</sub> nanoparticles on the cotton fabric. The effects of catalyst type (ammonia or HCL), MTEOS/ethanol and TMCS/ethanol volumetric ratio on the surface contact angle, air permeability, tensile strength and wash durability are investigated. The most appropriate condition for nanoparticles size and distribution belongs to the sample with 1 mL of MTEOS when ammonia is used as the catalyst solution. With increasing the amount of MTEOS from 0.5 mL to 2 mL, an increasing trend is observed in the contact angle. However, higher amount of precursor (2 mL) shows a reduction trend in the contact angle. Similar trend is observed in the contact angle of the samples with increasing the TMCS/ethanol ratio from 2.5 % vol to 5 % vol and then to 7.5 % vol. The samples prepared with ammonia catalyst solution exhibit

greater contact angles than the samples catalyzed by HCL solution. No significant change is observed in tensile strength and also in permeability of the samples after being coated in the first stage.

#### References

- 1 Yu S, Guo Z & Liu W, *Chem Commun*, 51 (2015) 1775. DOI: 10.1039/C4CC06868H.
- 2 Gogotsi Y, *Nanotubes and Nanofibers* (CRC Press), 2006.
- 3 Sepour S, *Nanotechnology: Technical Basics and Applications* (Vincentz Network GmbH & Co KG), 2008.
- 4 Solga A, Cerman Z, Striffler BF, Spaeth M & Barthlott W, *Bioinspiration Biomimetics*, 2 (2007) S126. DOI: 10.1088/1748-3182/2/4/s02.
- 5 Ganesh VA, Raut HK, Nair AS & Ramakrishna S, *J Mater Chem*, 21 (2011) 16304. DOI: 10.1039/C1JM12523K.
- 6 Li Y, Jia W-Z, Song Y-Y & Xia X-H, *Chem Mater*, 19 (2007) 5758. DOI: 10.1021/cm071738j.
- 7 Manoharan K & Bhattacharya S, *J Micromanuf*, 2 (2019) 59. DOI: 10.1177/2516598419836345.
- 8 Servinis L, Beggs KM, Scheffler C, Wölfel E, Randall JD, Gengenbach TR, Demir B, Walsh TR, Doeven EH, Francis PS & Henderson LC, *Carbon*, 118 (2017) 393. DOI: 10.1016/j.carbon.2017.03.064.
- 9 Stoica I, Barzic AI & Hulubei C, *Appl Surf Sci*, 426 (2017) 307. DOI: 10.1016/j.apsusc.2017.07.214.
- 10 Şimşek B & Karaman M, *J Coat Technol Res*, 17 (2020) 381. DOI: 10.1007/s11998-019-00282-7.
- 11 Ray SS, Chen S-S, Li C-W, Nguyen NC & Nguyen HT, *RSC Adv*, 6 (2016) 85495. DOI: 10.1039/C6RA14952A.
- 12 Abidi N, Hequet E, Tarimala S & Dai LL, *J Appl Polym Sci*, 104 (2007) 111. DOI: 10.1002/app.24572.
- 13 Li C, Iqbal M, Lin J, Luo X, Jiang B, Malgras V, Wu KCW, Kim J & Yamauchi Y, *Acc Chem Res*, 51 (2018) 1764. DOI: 10.1021/acs.accounts.8b00119.
- 14 Notsu H, Kubo W, Shitanda I & Tatsuma T, *J Mater Chem*, 15 (2005) 1523. DOI: 10.1039/B418884E.
- 15 Ma M, Mao Y, Gupta M, Gleason KK & Rutledge GC, *Macromolecules*, 38 (2005) 9742. DOI: 10.1021/ma0511189.
- 16 Brinker CJ & Scherer GW, *Sol-gel Science: The Physics and Chemistry of Sol-gel Processing* (Academic Press), 2013.
- 17 Basu BJ, Hariprakash V, Aruna ST, Lakshmi RV, Manasa J & Shruthi B S, *J Sol-Gel Sci Technol*, 56 (2010) 278. DOI: 10.1007/s10971-010-2304-8.
- 18 Lakshmi RV, Bharathidasan T & Basu BJ, *Appl Surf Sci*, 257 (2011) 10421. DOI: 10.1016/j.apsusc.2011.06.122.
- 19 Wang J, Chen J, Jin Z, Gu X, Zhang R, Huang J & Luo G, *Proceedings, 2nd International Conference on Civil, Materials and Environmental Sciences* (CMES 2015, London, UK) 2015, 651.
- 20 Jiang Z, Fang S, Wang C, Wang H & Ji C, *Appl Surf Sci*, 390 (2016) 993. DOI: 10.1016/j.apsusc.2016.08.152.
- 21 Taurino R, Fabbri E, Pospiech D, Synytska A & Messori M, *Prog Org Coat*, 77 (2014) 1635. DOI: 10.1016/j.porgcoat.2014.05.009.
- 22 Zhang M, Wang S, Wang C & Li J, *Appl Surf Sci*, 261 (2012) 561. DOI: 10.1016/j.apsusc.2012.08.055.
- 23 Colleoni C, Guido E, Migani V & Rosace G, *J Ind Text*, 44 (2015) 815. DOI: 10.1177/1528083713516664.
- 24 Das I & De G, *Sci Rep*, 5 (2015) 18503. DOI: 10.1038/srep18503.



- 25 Aqueous and Nonaqueous Sol-Gel Chemistry. *Metal Oxide Nanoparticles in Organic Solvents: Synthesis, Formation, Assembly and Application* (Springer London), 2009, 7.
- 26 Venkateswara Rao A, Latthe SS, Nadargi DY, Hirashima H & Ganesan V, *J Colloid Interface Sci*, 332 (2009) 484. DOI: 10.1016/j.jcis.2009.01.012.
- 27 Mohamed AMA, Abdullah AM & Younan NA, *Arabian J Chem*, 8 (2015) 749. DOI: 10.1016/j.arabjc.2014.03.006.
- 28 Petcu C, Nistor CL, Purcar V, Cintează LO, Spătaru C-I, Ghiurea M, Ianchiș R, Anastasescu M & Stoica M, *Appl Surf Sci*, 347 (2015) 359. DOI: 10.1016/j.apsusc.2015.04.073.
- 29 Shi Y, Wang Y, Feng X, Yue G & Yang W, *Appl Surf Sci*, 258 (2012) 8134. DOI: 10.1016/j.apsusc.2012.05.008.
- 30 Liu F, Ma M, Zang D, Gao Z & Wang C, *Carbohydr Polym*, 103 (2014) 480. DOI: 10.1016/j.carbpol.2013.12.022.
- 31 Kim C-Y & Jang AR, *Asian J Chem*, 24 (2012) 4217.
- 32 Vidal K, Gómez E, Goitandia AM, Angulo-Ibáñez A & Aranzabe E, *Coatings*, 9 (2019) 627.
- 33 Espanhol-Soares M, Costa L, Silva MRA, Soares Silva F, Ribeiro LMS & Gimenes R, *J Sol-Gel Sci Technol*, 95 (2020) 22. DOI: 10.1007/s10971-020-05307-x.
- 34 El-Bisi M, Ibrahim H, Rabie A, Elnagar K, Taha G & El-Alfy E, *Der Pharma Chemica*, 8 (2016) 57.
- 35 Mansor A, Ghani SA & Yahya MF, *Am J Mater Sci*, 6 (2016) 147.